Available online at www.sciencedirect.com
ScienceDirect
Polymer 48 (2007) 5289–5302
polymer
www.elsevier.com/locate/polymer

Anisotropy and instability of the co-continuous phase morphology in uncompatibilized and reactively compatibilized polypropylene/polystyrene blends

T.S. Omonov [a], C. Harrats [b], G. Groeninckx [b,*], P. Moldenaers [a,**]

[a] *Katholieke Universiteit Leuven, Department of Chemical Engineering, Division of Applied Rheology and Polymer Processing, W. De Croylaan 46, 3001 Heverlee, Belgium*

[b] *Katholieke Universiteit Leuven, Department of Chemistry, Division of Molecular and Nanomaterials, Laboratory of Macromolecular Structural Chemistry (MSC), Celestijnenlaan 200 F, 3001 Heverlee, Belgium*

Received 5 December 2006; received in revised form 19 June 2007; accepted 20 June 2007
Available online 26 June 2007

Abstract

The present work describes the anisotropy and instability observed upon the formation of co-continuous phase morphologies in model polystyrene/polypropylene melt-extruded blends. Uncompatibilized and reactively compatibilized blends using amino-terminated polystyrene, PS−NH_2, and maleic anhydride grafted polypropylene, PP−MAh, reactive precursors were investigated. Differences in phase morphology are discussed based on the viscoelastic properties of the components used, the blend composition and, the type and content of the compatibilizer precursor employed. As expected, for the same polystyrene grade at a concentration in the blend below 20 wt%, a polypropylene matrix having a higher viscosity enables the formation of a more co-continuous phase morphology than a less viscous one, as quantified by solvent extraction. The co-continuous phase morphology developed was found to exhibit a highly elongated structure upon melt flow through the die of the extruder. Isotropic co-continuity, observed inside the barrel of extruder, was transformed into anisotropic phase co-continuity in the form of interconnected infinite strands of the minor phase highly oriented in the extrusion direction.

When the blends were thermally annealed, a 50/50 PS/PP co-continuous blend exhibits a substantial phase coarsening from micro- to millimeter scale without alteration of the phase co-continuity. The reactive compatibilization of the polypropylene and the polystyrene phases using 5 wt% PP-*graft*-PS, reactively *in situ* generated was able to significantly retard the phase evolution process.

Keywords: Co-continuous phase morphology; Polypropylene/polystyrene blends; Phase anisotropy and stability

1. Introduction

The properties of immiscible polymer blends are to a large extend controlled by their phase morphology [1,2]. Two major phase morphologies can be distinguished in binary two-phase blends: isolated particles dispersed in a matrix and a two-phase co-continuous morphology. In the former, isolated droplets, platelets, rods or fibers of one phase are distributed in the matrix phase. The co-continuous two-phase morphology consists of two-coexisting, continuous and interconnected phases throughout the whole blend volume. In polymer blends having a dispersed phase morphology the properties are mainly controlled by the matrix, except in rubber toughening of brittle matrices where the morphology, i.e., size, volume fraction and spatial distribution of the dispersed phase is a key factor in inducing toughness [3]. In contrast, in a co-continuous two-phase morphology the two components contribute simultaneously to the properties of the blend. Co-continuous nano- to micro-phase morphologies can be generated from partially miscible blends during the spinodal demixing process, whereas, co-continuous micro- to macro-phase morphologies

* Corresponding author. Tel.: +32 16 32 74 40; fax: +32 16 32 74 90.
** Corresponding author. Tel.: +32 16 32 23 59; fax: +32 16 32 29 91.
E-mail addresses: gabriel.groeninckx@chem.kuleuven.be (G. Groeninckx), paula.moldenaers@cit.kuleuven.be (P. Moldenaers).

0032-3861/$ - see front matter © 2007 Elsevier Ltd. All rights reserved.
doi:10.1016/j.polymer.2007.06.043

can be developed via melt-blending of immiscible polymers under well defined conditions of blend composition, component characteristics and machine parameters.

Co-continuous phase morphologies, developed in a binary immiscible polymer blend upon melt-mixing, remain poorly understood. The first challenge met is associated with the prediction of the conditions, in terms of composition and viscoelastic properties of the blend components, at which phase inversion occurs. Various empirical relations have been proposed; they usually include the volume fraction of the individual blend phases and their viscosity ratio [4–13]. Unfortunately, none of the empirical relations has been generally successful in predicting the experimental observations. The debate continues about the possibility of deriving a universal relation to predict the conditions at which phase inversion occurs. The concept of phase inversion has become of secondary importance since it is now known that a co-continuous phase morphology develops over a wide composition window which can be as broad as 0.2–0.8 volume fraction range of one component [14].

The second challenge associated with the development of a co-continuous phase morphology is related to its stability when subjected to various treatments such as thermal annealing above the melting or softening temperatures of the individual components in quiescent conditions [15–20] or their re-processing in extruders at various shear rates [21–26]. For practical applications, the extruded blends should be processable under various conditions without significant evolution of the co-continuous structure and without phase coarsening. A narrowing of the co-continuous composition range upon thermal annealing in the melt-state has been reported in literature [22,27–29]. This is caused by a significant and faster break-up process of the longer and thinner threads that constitute the co-continuous structure at lower contents of the minor phase. This suggests that there exists a critical volume fraction Φ_{cr} above which the co-continuous structures do not break-up during the melt-annealing. Willemse [22,30] related this volume fraction to the length of the threads between two neighboring nodes of the structure. No break-up will occur as long as this length is smaller than the wavelength of a sinusoidal disturbance. Another process of phase morphology instability resides in the phase coarsening upon thermal annealing. The rate of phase coarsening of a co-continuous phase morphology depends on temperature and on the characteristics of the components such as the interfacial tension and viscosity. Veenstra et al. [31] proposed an equation to predict the phase coarsening upon thermal annealing in quiescent conditions based on the effective viscosity η_e, (weight average of the zero shear rate viscosities of the components) as: $dr/dt = c\sigma/\eta_e$, where dr/dt is the average thickness of the network strands changing with time, c is a dimensionless factor depending on the volume fraction of the blend component and σ is interfacial tension.

Harrats et al. [15,20] reported earlier that a physically added copolymer based on hydrogenated polybutadiene and polystyrene had a significant effect on the stability of the co-continuous phase morphology in a model blend of polystyrene and polyethylene. Substantial differences were found between a tapered diblock HPB-*b*-PS, a pure diblock and a triblock copolymers. The tapered copolymer was able to stabilize the co-continuous phase morphology more efficiently than either the pure diblock or the triblock. Addition of SEBS triblock copolymer caused a shift in the percolation concentration of PS particles to higher values, and resulted in a narrower co-continuous composition window [32–34]. Galloway et al. showed that an intermediate molecular weight of PS–PE block copolymer (40 kg/mol) had a remarkable effect on reducing the phase size and stabilizing the blend morphology during thermal annealing compared to a low (6 kg/mol) and high (100 and 200 kg/mol) molecular weight block copolymers. This was ascribed to a molecular weight balance between the ability of the block copolymer to reach the interface and its relative stabilization effect at the interface [35]. Reactively compatibilized blends were also reported to exhibit a shift in co-continuous range compared to noncompatibilized blends [25,36,37].

In the present study, the phase morphology of PP/PS model blends, uncompatibilized and reactively compatibilized using amino-terminated polystyrene and maleic anhydride grafted polypropylene reactive precursors, is experimentally investigated. The focus is put on the study of stability and/or evolution of the co-continuous phase morphology during extrusion melt-blending. The work is an extension of the recently reported results on the significant extent of anisotropy observed in co-continuous binary blends having an asymmetrical composition (blends composed of a minor and a major phase) [14].

2. Experimental

2.1. Materials and blend preparation

The pure polymers used in the present investigation are two types of polypropylene (PP12 and PP37) from Borealis, having different melt flow indexes (MFI), and two polystyrenes, PS 158K from BASF and Styron 660-7 from Dow (PS3 and PS7). The reactive precursors used for the *in situ* formation of polystyrene-*graft*-polypropylene (PP-*g*-PS) copolymer at the interface of the PP and PS blend phases are amino-terminated polystyrene PS–NH_2 (P3695-SNH2) from Polymer Source and two maleic anhydride grafted polypropylene grades, Orevac OE708 from Atofina and Epolene E43 from Eastman Kodak, having a maleic anhydride content of 1.0 and 7.8 wt%, respectively. The homopolymers and compatibilizer precursors used are listed in Table 1. The codes for the compatibilizer precursors are based on their maleic anhydride (MA) content as PP–MA1 (1 wt% MA) and PP–MA8 (7.8 wt% MA). Two concentrations, 1 and 5 wt% of the *in situ* generated PP-*g*-PS compatibilizer with respect to the total blend, were investigated. Note that the ratio of [PP + (PP–MA)] to [PS + (PS–NH_2)] in the compatibilized blends was kept constant in the various blend compositions used. For the compatibilized blends a ratio of PP–MA to PS–NH_2 is fixed based on a stoichiometric concentration of reactive

Table 1
Properties of the homopolymers and compatibilizer precursors used

Material	MFI g/10 min	Material code	Structure	Supplier
PP (230 °C, 2.16 kg)	12.0	PP12	Homopolymer	"Borealis"
	37.0	PP37		
PS 158 K (200 °C, 5 kg)	3.0	PS3	Homopolymer	"BASF"
PS Styron 660-7 (200 °C, 5 kg)	7.0	PS7	Homopolymer	"Dow"
PS–NH_2, P3695-SNH2	–	PS–NH_2	NH_2 terminated, f > 0.95%	"Polymer Source"
PP-*g*-MA1, Orevac OE708	–	PP–MA1	MA grafted, 1 wt%	"Atofina"
PP-*g*-MA8, Epolene E43	–	PP–MA8	MA grafted, 7.8 wt%	"Eastman Kodak"

functionalities i.e. a ratio of amine to anhydride group of 1 is maintained throughout.

The blends were prepared by means of a midi-extruder (DSM Research) having a total mixing capacity of 15 cm^3. The mini-extruder can function as an internal mixer where the mixing time can be varied freely via a re-circulating internal channel. All the blends were prepared according to the same experimental procedure. The mixing temperature was fixed at 215 °C. In a typical blending operation PS and PP homopolymers and the compatibilizer precursors are fed into the extruder as a dry mixture under nitrogen flux at a screw rotation speed of 50 rpm. When all blend components were completely fed into the extruder, the rotation speed was increased to 100 rpm and the melt was blended for 10 min.

2.2. Phase morphology characterization

To determine the composition window in which the blends exhibit a droplet-in-matrix phase morphology and where the two phases are co-continuous, samples of known weight (taken from extruded strands with a thickness of 2–3 mm) of each blend were stirred in chloroform for 7 days to selectively extract the PS phase. The phase co-continuity index (CCI) of PS phase was quantified as the percentage of the polystyrene phase that was extracted using Eq. (1):

$$\mathrm{CCI_{PS}} = \frac{m_{or} - m_{ex}}{m_{or}} \cdot 100\% \quad (1)$$

where m_{or} is the weight of PS phase originally present in the blend, and m_{ex} the weight of PS phase in the blend after solvent extraction. It has been verified whether the sample preserved its shape or 'disintegrated' totally or partially into polypropylene particles. In case of the sample being not disintegrated, the polypropylene phase was considered as 100% continuous, provided that no non-soluble particles were depicted in the solvent, and the continuity of PS was quantified from the weight of the extracted part. If the sample fragmented, the weight ratio of the biggest piece with respect to the PP content was taken as the percentage of PP continuity based on the percolation principle. If the sample was completely disintegrated, then the PP phase was considered as fully dispersed in the PS matrix.

The phase morphology of the PP/PS blends was observed by SEM (Philips XL 20 Series) on gold coated surfaces. The observed surfaces were both cryo-smoothed using a Leica Ultracut UCT cryo-microtome at −100 °C and etched using chloroform or cryo-fractured in liquid nitrogen. The size of the minor PS phase was computed from the SEM micrographs using Leica QWin image analysis software.

2.3. Rheology

The rheological characterization of the pure polymers was carried out on a stress controlled rheometer from Rheometric Scientific (DSR200) using cone-plate geometry. Samples with a diameter of 25 mm and a thickness of 1 mm were compression moulded from the test material using a Collin press at a temperature of 205 °C. The measurements were performed at 205 °C under nitrogen atmosphere. The frequency was varied from 100 to 0.06 rad/s and the strain amplitude was kept small enough (5%) to ensure a linear viscoelastic response of the polymers. Fig. 1 represents the complex viscosities and storage moduli of the PP (a) and PS (b) homopolymers as a function of frequency at a temperature of 205 °C.

3. Results and discussion

3.1. Co-continuous phase morphology in noncompatibilized PP/PS blends

3.1.1. Phase co-continuity versus viscous properties of the blend components at low polystyrene content

In Fig. 2 the co-continuity index is plotted as a function of the polystyrene content for two polypropylene grades having complex viscosities of 406 Pa s (PP12) and 260 Pa s (PP37) at 100 prad/s and 205 °C. Each PP grade is melt-blended individually with a polystyrene grade having a viscosity of 863 Pa s (PS3) or 660 Pa s (PS7). Substantial differences are clearly visible at low PS content between the two series of blends.

The onset of PS phase continuity is found to depend on the viscosity of both PP and PS phases. The composition window at which the investigated blends exhibit almost 100% co-continuity covers a wide range from 30 to 90 wt% PS. However, substantial differences between the blends are observed outside this range (see data points at 10 wt% PS). The polystyrene phase is less co-continuous in the polypropylene matrix having a viscosity of 260 Pa s (PP37) than in the one having 406 Pa s (PP12).

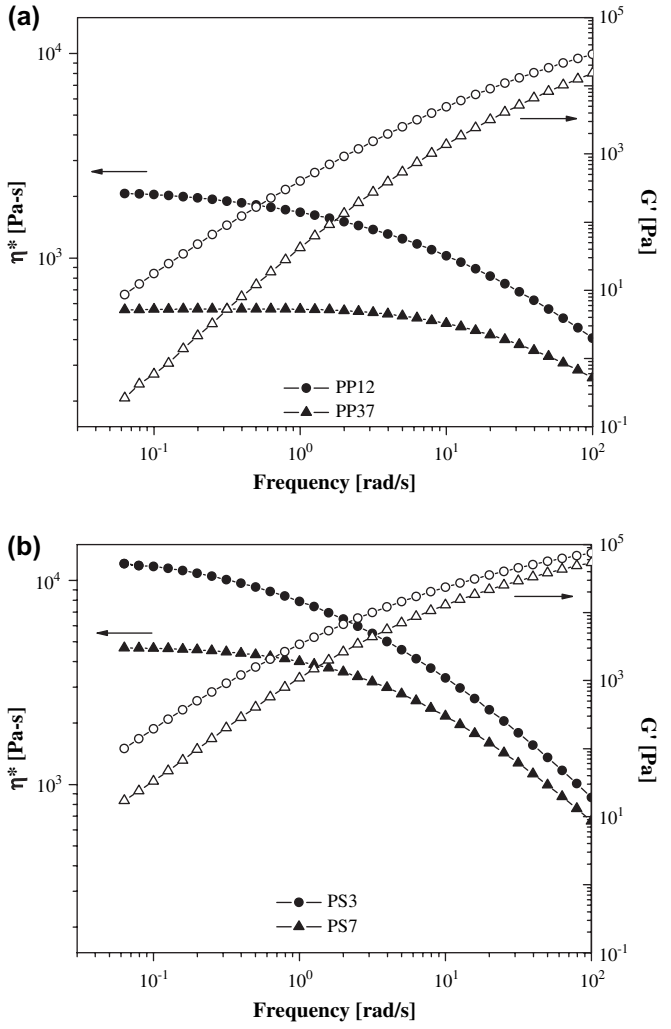

Fig. 1. Complex viscosity and storage modulus of the PP and PS homopolymer grades as a function of frequency (filled symbols: complex viscosity, open symbols: storage modulus).

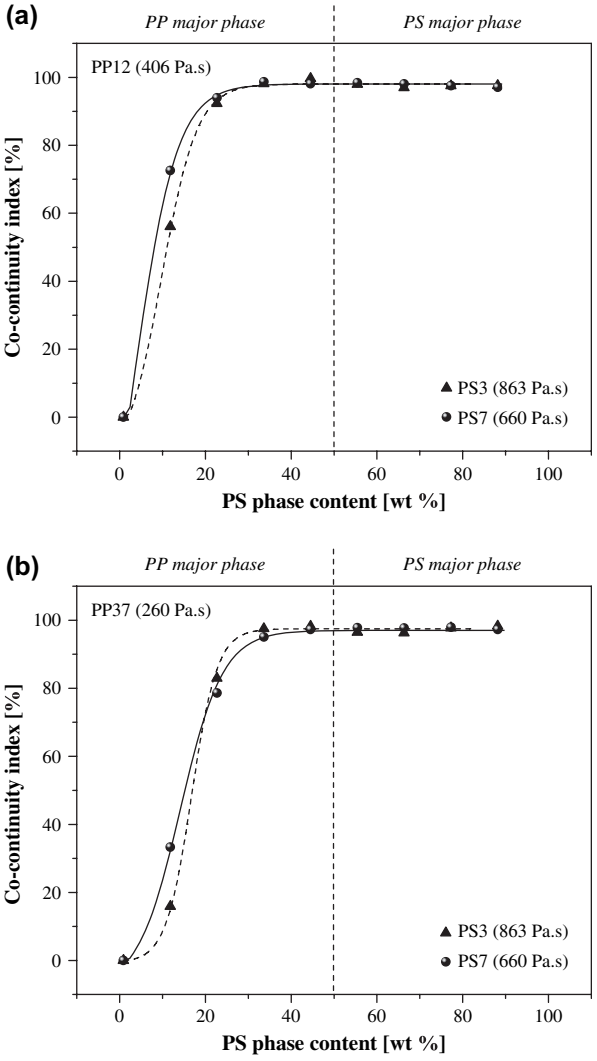

Fig. 2. Phase co-continuity index as a function of PS content in PP/PS blends composed of grades with different viscosities (a – PP12, b – PP37 as a basic phase, vertical dashed line shows the phase majority), viscosities are values at 100 rad/s.

Few models have been proposed in literature for the prediction of phase co-continuity using the viscosity ratio [5–7] or torque ratio during melt-blending [4,8]. These models do not take into account the shear history effects and requirements to the shape of the minor phase. In order to have a co-continuous system at low concentrations of the minor phase, the minor phase should be present in a shape of elongated rod-like structure [24,14]. As can be seen from Fig. 2, at all combinations of viscosity ratio of the minor to major phases, the lower limit for phase co-continuity is found at as low as 10 wt% PS. Table 2 shows the viscosity ratio of PS and PP homopolymers at 100 rad/s. The viscosity ratios of the blend components used in the preparation of the blends under investigation are ranging from 1.6 to 3.3.

As can be seen from Fig. 2(a), the blends composed of PP12 and PS7 having a viscosity ratio of 2.1 result in a co-continuous structure of about 73% at a composition of 90/10 PP/PS. When using a high viscosity PS3 grade a drop in the extent of co-continuity is observed at the same PS content (10 wt%) from 73% to 56%. The use of PP37 having a lower viscosity as a major phase lead to a substantial decrease of phase co-continuity (33% for PS7, 16% for PS3). It can be concluded that increasing the matrix viscosity leads to a more stable elongated structure of the minor phase, allowing to obtain a more quantitative value of co-continuity at low volume fractions of the minor phase [24].

3.1.2. Phase morphology development

To investigate in more detail the phase morphology development during the melt-blending in the twin-screw mini-extruder, the blends based on PP12 and PS7 homopolymers

Table 2
Viscosity ratio for the components at 100 rad/s, 205 °C

$\eta^*_{PS3}/\eta^*_{PP12}$	$\eta^*_{PS3}/\eta^*_{PP37}$	$\eta^*_{PS7}/\eta^*_{PP12}$	$\eta^*_{PS7}/\eta^*_{PP37}$
2.12	3.32	1.63	2.55

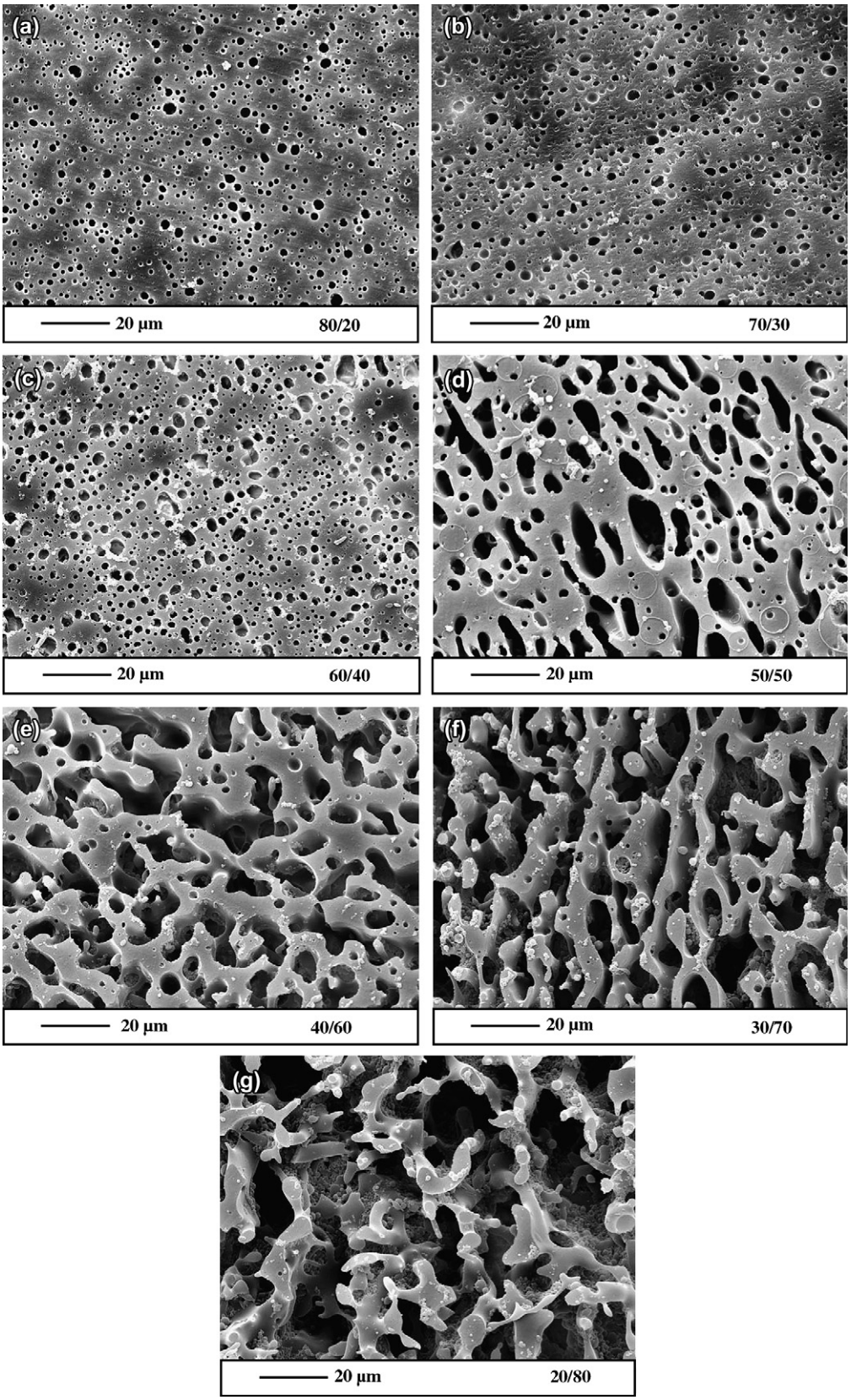

Fig. 3. SEM micrographs of cryo-smoothed and chloroform etched surfaces of PP12/PS7 blends observed in perpendicular to extrusion direction.

were selected. The SEM micrographs of the cryo-smoothed surfaces obtained from the co-continuous blends having the compositions between 80/20 and 20/80 are shown in Fig. 3. The surfaces observed were cut from the extruded strands in a plane perpendicular to the extrusion direction. The polystyrene phase was selectively extracted using chloroform. Two apparent phase morphologies are distinguishable in this plane: the four blends having a polystyrene content below 50 wt% consist of polystyrene droplets dispersed in a polypropylene matrix, whereas both phases are co-existing in a coral-like interconnected network structure in the blends containing larger amounts of polystyrene. The size of the polystyrene domains decreases as the content of polystyrene phase is reduced like in a purely dispersed phase morphology. This is due to an enhanced coalescence process when the concentration of the dispersed phase is large. The most striking observation is that the morphologies observed in perpendicular plane are actually fully co-continuous, as revealed by the extraction experiments. Similar observations were reported elsewhere [14].

The SEM investigation of the phase morphology of PP12/PS7 blends in the longitudinal direction parallel to the extrusion direction reveals a pronounced anisotropy as can be seen from the corresponding SEM micrographs of the cryo-fractured surfaces in Fig. 4. An extensive orientation of the polystyrene phase in the extrusion direction is obvious in contrast with the apparent particle-in-matrix phase morphology observed in a perpendicular plane. The apparent polystyrene droplets observed in the perpendicular direction turn out to be connections and ends of polystyrene rods. It can be concluded that the phase co-continuity is preserved although the polystyrene phase is highly oriented, thus generating an anisotropic co-continuous phase morphology. Even in the morphologies, which are coral-like in the perpendicular plane, an extensive minor phase orientation took place upon melt-extrusion. However, as evidenced in the SEM micrographs of Fig. 4(d)–(f), the oriented structures are not rod-like in shape but look like infinite flat platelets. These flat plate-like shapes are also visible, for example, in the perpendicular cut in Fig. 3(f).

As reported earlier [14], co-continuity is possible not by with standing the presence of highly anisotropic phase constituted of infinitely long entities, but because of interconnections as indicated on the SEM micrographs of Fig. 4(a) and (c). Note that the white arrows indicate the direction of the flow in the extrusion process. A co-continuous morphology can be found in the samples if the break-up time of the elongated interconnected domains is much shorter than a characteristic quench time. To check whether these morphologies are resulting from orientation as induced by the capillary of the die, samples where picked-up from inside the barrel by opening the extruder. The SEM observation reveals, as shown in Fig. 5, that the phase morphology generated inside the extruder is mostly similar in all directions (not shown here) but differs substantially from those after flowing through the die (see Fig. 3). After the quantification of the co-continuity of the PS phase with a solvent extraction procedure, it appears that we have a case of orientation-induced co-continuity (Fig. 6).

Note that the full co-continuity region of these blends occurs within a narrow composition range of 40–70 wt% of PS phase, whereas the same blends after melt flow through the die exhibit a co-continuity in as large as a composition range of 30–90 wt% of PS. Dispersed 20/80, 10/90, and 90/10 PP/PS compositions were converted to co-continuous blends via flow through the die of the extruder. The phenomenon is observed when the two situations are compared: i.e. before the entrance into the die and after the exit from the die of the extruder. The SEM micrographs in Fig. 4(a)–(c) illustrate an extensive orientation of the minor phase, where interconnections of the elongated entities are clearly visible.

3.1.3. Phase morphology stability

The blends having a composition of 20/80 PP/PS, which have a fully co-continuous phase morphology and are situated at the edge of the composition window of co-continuity are good to study the extent of phase stability upon thermal annealing.

SEM micrographs of the cryo-smoothed and solvent extracted surfaces of extruded strands of this blend cut parallel and perpendicular to the flow direction are shown in Fig. 7. It is interesting to see that SEM micrographs of the perpendicular cut surfaces reveal a radial orientation of the domains (Fig. 7(a)). Away from the center and near the border of the strand, the PP phase becomes elongated and orientation increases due to the high shear rate at the wall of the die (Fig. 7(b) and (c)). In the surfaces cut parallel to the flow direction (Fig. 7(a′)), particularly in the middle of the strand where the shear rates are the lowest, less elongated rod-like fibrils of the PP phase can be seen as shown in Fig. 7(b′). Furthermore, a highly oriented and coral-like skeletal structure can be observed close to the border of the strand (Fig. 7(c′)). One can conclude that the co-continuous phase morphology at the border of the co-continuity composition window is very sensitive to changes in shearing forces.

To study the stability of the developed co-continuous phase morphology upon thermal annealing in the absence of shear, two compositions were selected: 20/80 and 50/50 PP/PS situated at the boundary and in the mid-range of the co-continuity composition window, respectively. As shown in Figs. 8 and 9, the two blends responded differently to the thermal annealing treatment at 205 °C. When the 20/80 PP/PS (Fig. 8) is annealed at 205 °C during 5, 10, 20 and 40 min, the co-continuity is completely altered resulting in a fully dispersed phase morphology. Note that after as short as 5 min the phase evolution is total and no further change is observed for larger time periods. This is an additional proof of the instability of the co-continuous phase morphology. A close observation of the pictures in Fig. 8 reveals bimodal size distribution of the PS particles (big generation of particles and very small major generation). This is the result of a particular process associating both fiber break-up and retraction. The break-up of a modulated co-continuous morphology would be driven by the surface

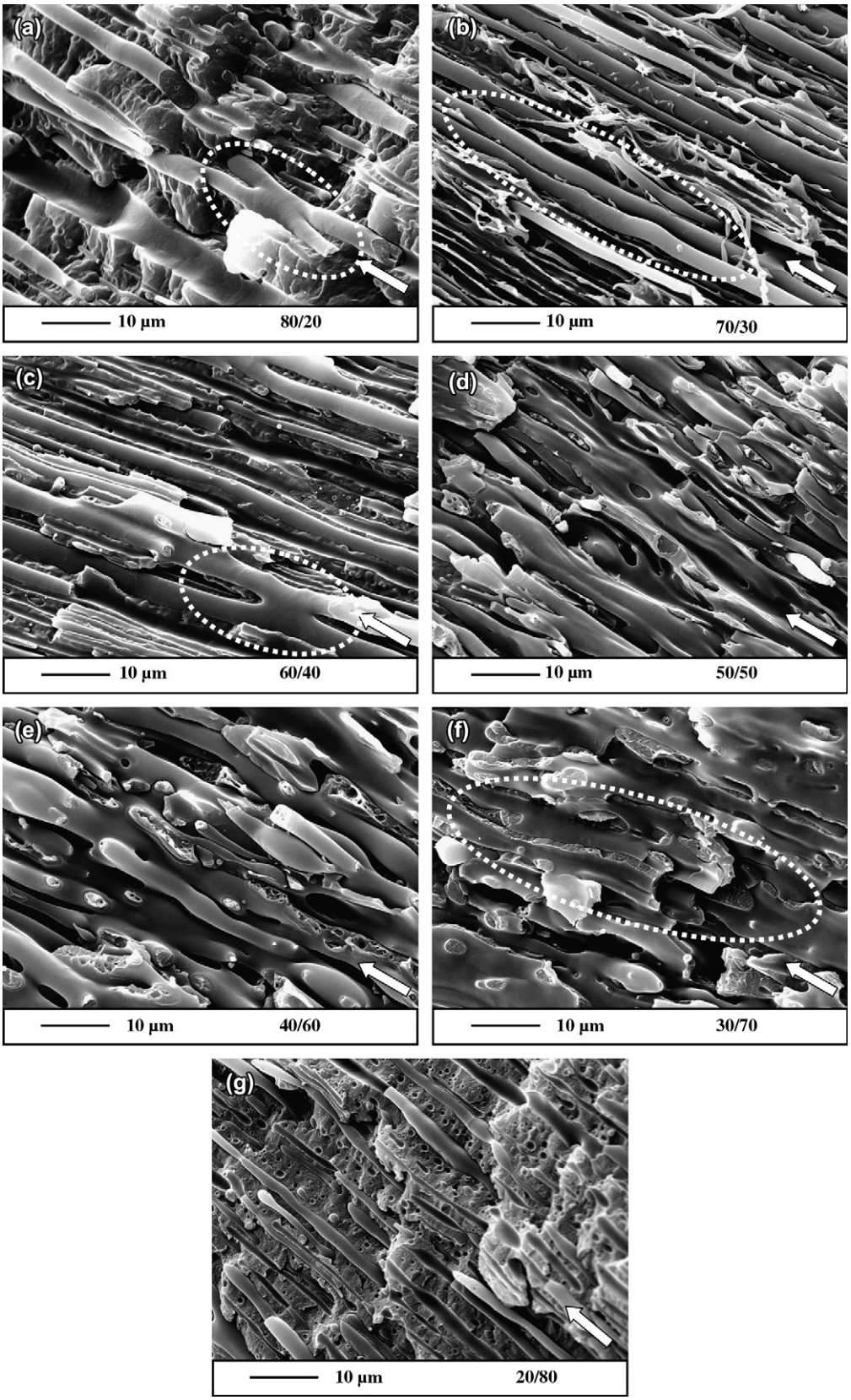

Fig. 4. SEM micrographs of cryo-fractured surfaces of PP12/PS7 blends observed in the direction parallel to extrusion.

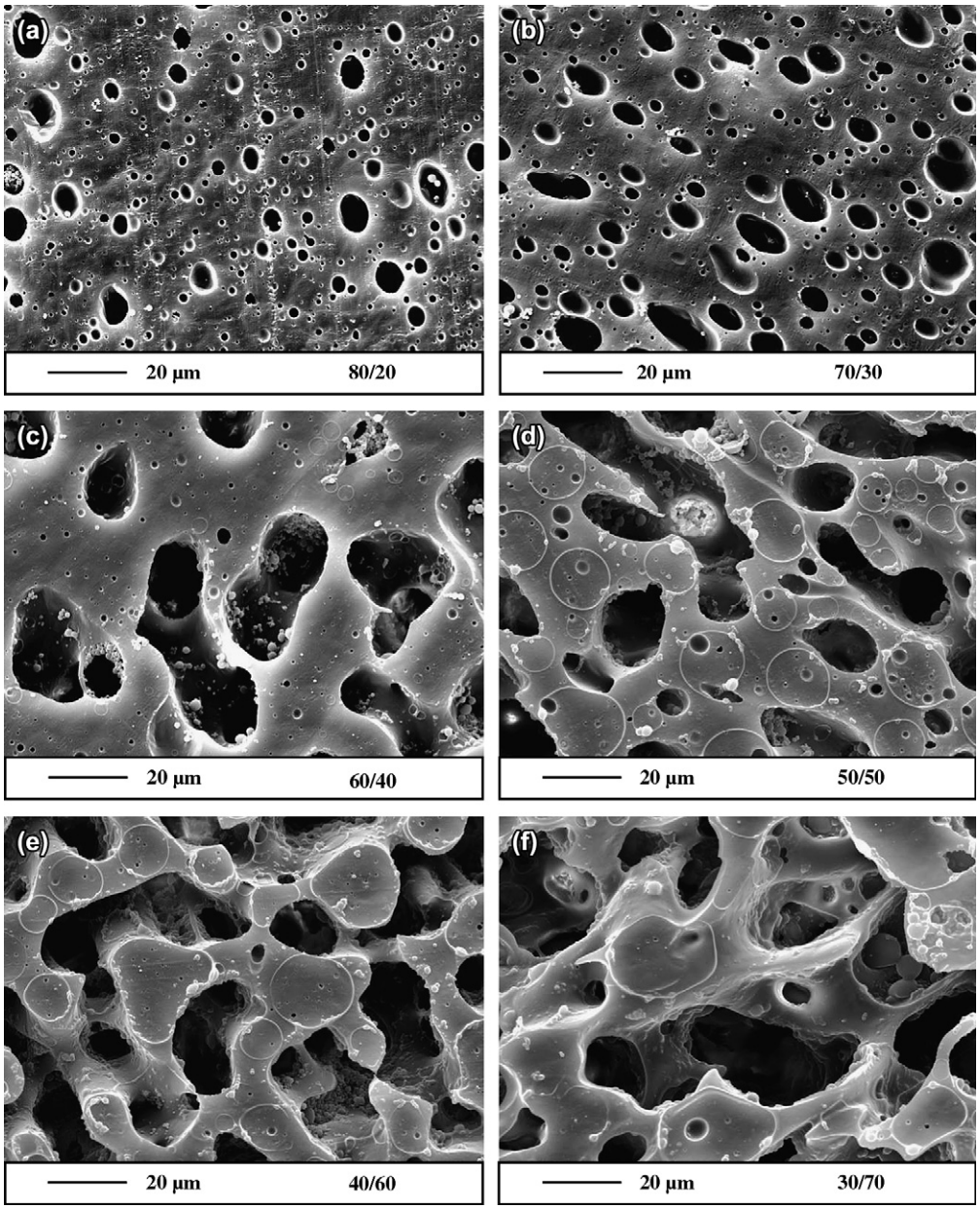

Fig. 5. SEM micrographs of cryo-smoothed and chloroform etched surfaces of PP12/PS7 blends picked-up from inside the barrel of the extruder (before die entrance).

tension, which in turn generates a pressure gradient causing flow from the thin part to the thick part of the structure [38,39]. Willemse et al. [40] also found that in a melt-blended co-continuous structure, where the volume fraction of one of the phases is much lower than the other, coarsening of the phase morphology was attributed to a restructuring process involving fiber retraction and break-up. At higher volume fractions (>30 vol%), both major and minor components belong to an interconnected network structure, and coarsening in these co-continuous structures occurs by the retraction mechanism only.

On the other hand, when the 50/50 blend is considered, thermal annealing was not able to alter the co-continuous structure of the blend but could coarsen it substantially to a different degrees depending on the annealing time (Fig. 9, top row for uncompatibilized blend).

3.2. Phase morphology in compatibilized PP/PS blends using reactive precursors

Fig. 9 shows the effect of the type and content of the *in situ* generated reactive compatibilizer PS-*g*-PP on the co-continuous phase morphology of the compatibilized 50/50 PP/PS blend. The first column shows the initial phase morphology of the as-extruded blends, before annealing. The reactive compatibilization does not seem to have a significant effect on the final morphology of the blends as extruded. Only in the case of 5 wt% compatibilizer, generated using the precursors PP–MA8 and PS–NH_2, a more tortuous and fine texture of the phase morphology is formed. Furthermore, a close observation of the SEM micrographs reveals that two populations of pores co-exist, resulting in a bimodal pore

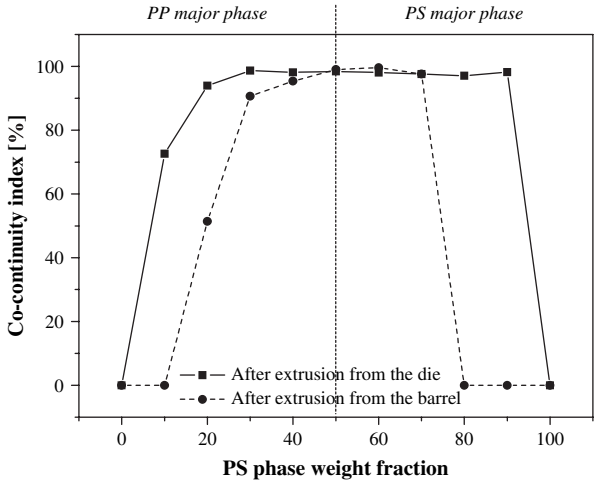

Fig. 6. Effect of flow conditions on co-continuity index of PP12/PS7 blends as a function of PS content.

distribution over the observed surfaces. Note that these blends exhibit an extensive anisotropy due to the orientation caused by the flow through the die of the extruder (Fig. 4(d)).

The compatibilizer shows a clear effect in retarding the coarsening of the phases, when the 50/50 PP/PS blend is annealed at 205 °C (Fig. 9, columns 2–5). Similar effects were reported by Harrats et al. [15,20] on compatibilized polyethylene/polystyrene blends using a physical compatibilizer of hydrogenated polybutadiene-*b*-polystyrene copolymer. Note that the copolymer reactively formed from PP–MA1 and PS–NH_2 is less efficient than that formed reactively from PP–MA8 and PS–NH_2. The former only moderately inhibits the coarsening of the PS phase. In contrast, the PP–MA8 based copolymer was able to completely suppress the evolution of the phases leading to a stable co-continuous phase morphology even after 60 min of thermal annealing at 205 °C. From the solvent extraction data listed in Table 3, it can be conclude that nearly no PS particles are formed during the annealing process. That means that no multiple fiber break-up has occurred but fiber rupture at its thinnest diameter took place allowing for retraction of the divided parts and coalescence the mother PS phase structure.

To have a quantitative evaluation of the phase coarsening, a perimeter per area is measured from the SEM micrographs of the annealed blends. Fig. 10 shows a semi-logarithmic plot of the measured perimeter per area against the annealing time for the uncompatibilized and compatibilized blends. It is clear that the amount of the interface in the uncompatibilized blend is reduced dramatically from 1.6 to 0.07 μm^{-1} in 5 min of annealing time. A further annealing does not change significantly the situation (0.03 μm^{-1} after 20 min). Similar changes of interfacial area are observed for the blends containing 1 wt% of compatibilizer using PP–MA1 precursor. For the blend with 5 wt% compatibilizer, the change in interfacial area is slower than that for the uncompatibilized blend. However, after 20 min of annealing the phase morphology of this blend closely resembles that of the uncompatibilized blend. The blend with 1 wt% compatibilizer based on PP–MA8 shows an initial change similar to the previous blends, but the interfacial area was twice larger after 20 min of annealing. The most stable composition was that of the blend having 5 wt% compatibilizer based on the precursor combination of (PP–MA8) + (PS–NH_2). It exhibits the largest amount of interface at all annealing times. The phase coarsening levels off after 10 min of annealing applied (specific interfacial area of $\approx 0.2\ \mu m^{-1}$).

The Doi–Ohta theory for complex interfaces [41] was adapted by Vinckier and Laun [42] to the annealing of polymer blends, having a co-continuous phase morphology. Eq. (2) was derived for the calculation of the coarsening rate of co-continuous structures under a quiescent annealing procedure:

$$\frac{1}{Q} = \frac{1}{Q_0} + c_1 \frac{\sigma}{\eta} t \tag{2}$$

where Q_0 is the specific interfacial area prior to annealing ($t = 0$), c_1 the kinetic constant for size relaxation, σ the interfacial tension and η the viscosity of the blend (2685 Pa s for the PP/PS at 0.04 rad/s, 205 °C). An interfacial tension of 3.25 mN/m at 205 °C for PP/PS blends was calculated using surface tension values and polarities as described elsewhere [43–45]. Eq. (2) was used to obtain the coarsening rate values from the initial linear coarsening region based on the experimental data.

Fig. 11 represents the reciprocal of the specific interfacial area ($1/Q$) versus the annealing time for the blends of Fig. 10. The annealed blend with 5 wt% compatibilizer based on PP–MA8 has a final $1/Q$ value of 8.7 against 36.6 for the uncompatibilized blend, indicating the superior influence of this compatibilizer on stabilizing the co-continuous phase morphology during annealing. Kinetic constants for size relaxation multiplied with the interfacial tension ($c_1\sigma$) and normalized values with that of neat blends are summarized in Table 3. The values indicate again that the slowest coarsening rate is exhibited by the blend having 5 wt% compatibilizer based on PP–MA8.

The architecture and interfacial coverage of the compatibilizer are useful parameters for understanding the compatibilization efficiency of copolymers in immiscible polymer blends. Interfacial coverage, Σ for the co-continuous blends was estimated using [35]:

$$\Sigma = \frac{w_{cop}\rho_{cop}N_A}{QM_n} \tag{3}$$

where w_{cop} is the weight fraction of *in situ* formed graft copolymer, ρ_{cop} is the density of the graft copolymer, N_A is Avagadro's number, Q is the specific interfacial area and M_n is the number average molecular weight of graft copolymer. The density of the graft copolymers was estimated to be the average of the densities of PP (0.908 g/cm^3) and PS (1.05 g/cm^3), i.e. 0.979 g/cm^3, w_{cop} is either 0.01 or 0.05. Knowing the M_n of PP–MA8 (3.96 kg/mol) and measuring the viscosity of PP–MA8, the value of K can be derived

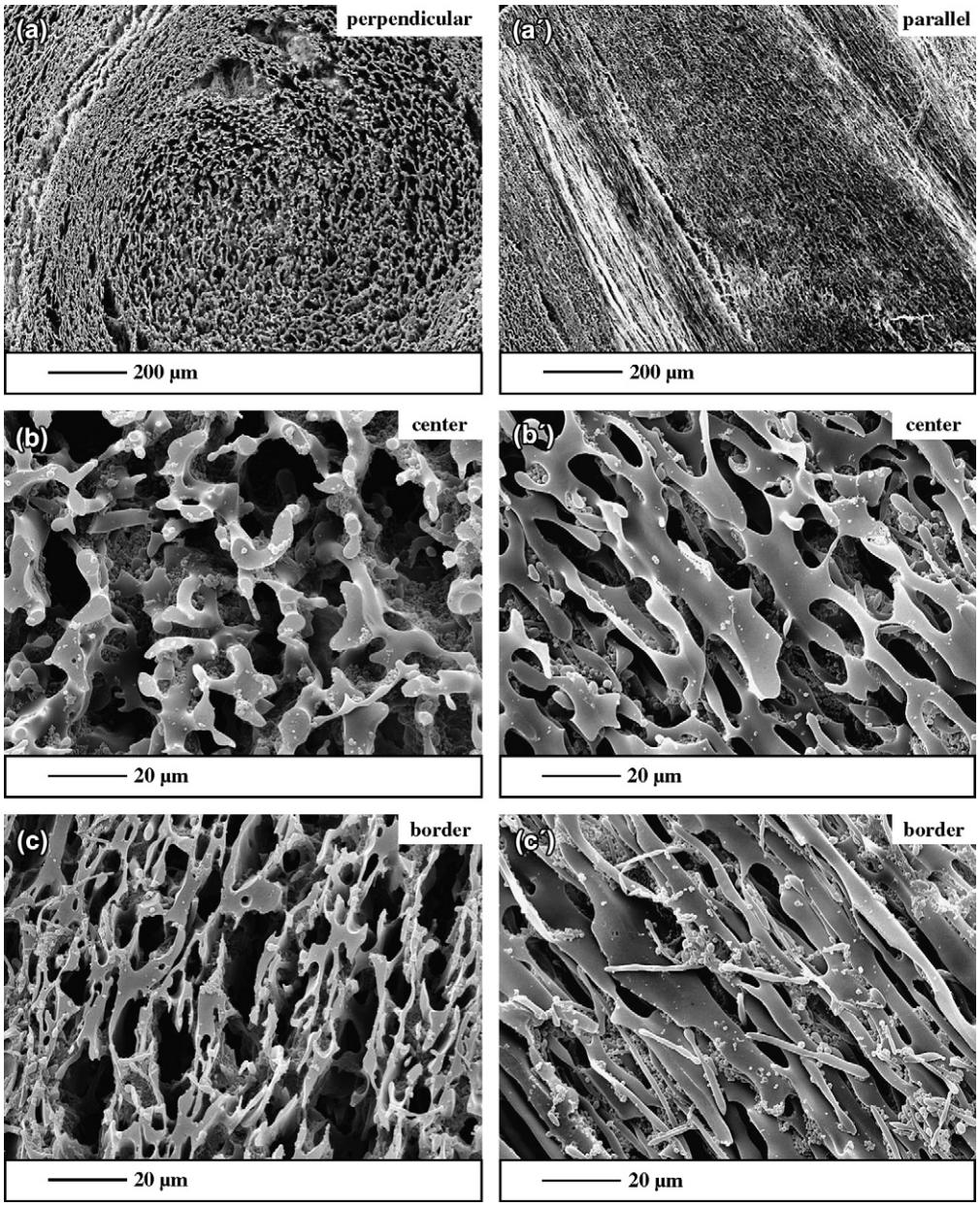

Fig. 7. SEM micrographs of PP12/PS7 20/80 blends: comparison of phase morphology in the perpendicular and parallel directions and at various positions in the sample.

from the equation $\eta = KM_n^{3.4}$ [45] ($K = 2.55 \times 10^{-3}$). Using this value of K, the M_n of PP−MA1 is estimated to be 60.0 kg/mol. The M_n of the *in situ* generated copolymers was estimated from the M_n of PP−MA1 or PP−MA8 and PS−NH_2 (10.0 kg/mol) precursors, 121.3 kg/mol for (PP−MA1) + (PS−NH_2) and 35.5 kg/mol for the combination of (PP−MA8) + (PS−NH_2). The ''average architecture'' of *in situ* generated graft copolymers is indicated in Fig. 12. Based on the stoichiometric concentration of the compatibilizer precursor, an average amount of PS−NH_2 pendant grafts per PP−MA1 and PP−MA8 backbone was estimated to be 6 and 3, respectively. It is assumed that all the copolymers generated reside at the interface (considering a low bulk solubility of the copolymers in the phases) and that no micelles are present in the system [46]. Hence Eq. (3) will give an apparent interfacial coverage (see Table 3).

A maximum interfacial coverage by block copolymers, Σ_{max}, can be calculated using a lamellar spacing assumption and a scaling factor [35,46]. The branched architecture of the graft copolymers, however, can result in a nonlamellar morphology even in a compositionally symmetric molecule, due to asymmetric interfacial crowding [47]. In our case, the concentration of branched graft copolymer necessary to saturate the interface can only be estimated using a scaling relation $\Sigma_{max} \sim M_n^{-1/3}$ [34,46]. It leads to 0.20 and 0.30 chain/nm^2 for the graft copolymer based on PP−MA1 and PP−MA8,

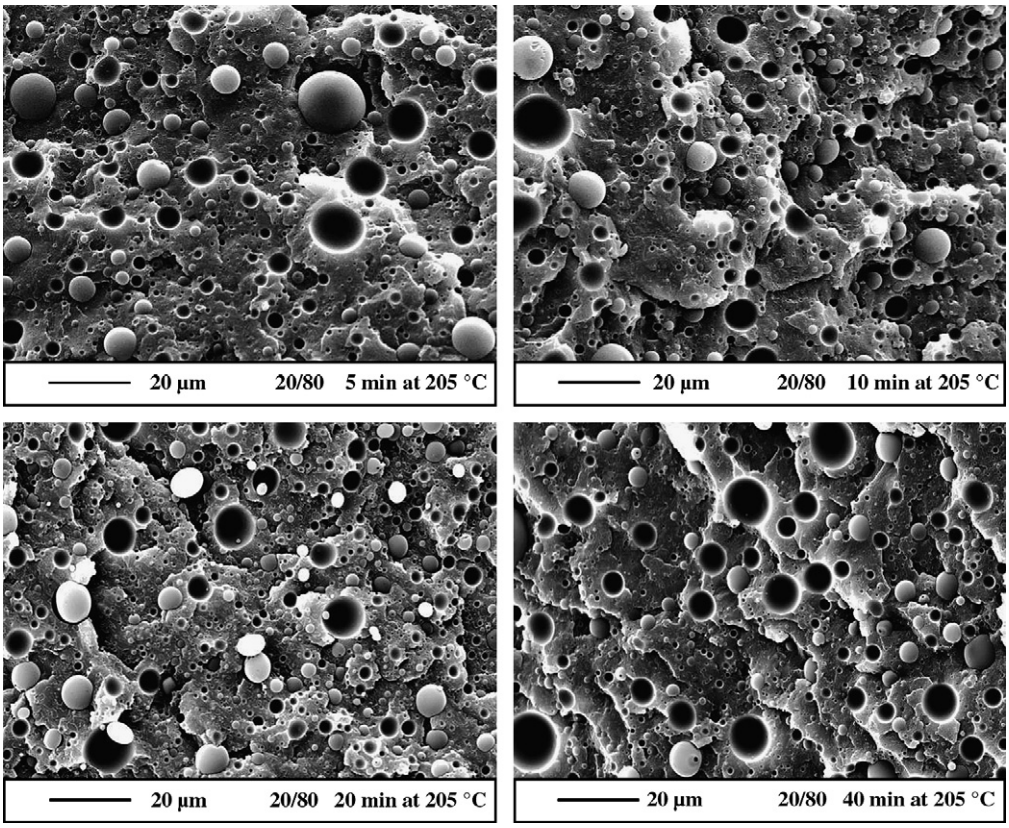

Fig. 8. SEM micrographs of cryo-fractured surfaces of PP12/PS7 20/80 blends: samples annealed at 205 °C for various time periods.

respectively. The ratio of Σ/Σ_{max} being below unity for the blends with 1 wt% of *in situ* generated copolymer, using PP–MA1 or PP–MA8 (see Table 3) suggests that this amount is not enough to saturate the interface during melt-blending. The blend with 5 wt% compatibilizer gives $\Sigma/\Sigma_{max} > 1$, which implies that the interface has been saturated during mixing.

Inefficiency of high molecular weight copolymers for compatibilization can be explained by a low diffusion mobility to the interface [48]. They can be trapped in micelles in the parent homopolymers. Relatively low molecular weight graft copolymers, based on PP–MA8 can easily reach the interface [49]. Nevertheless, we cannot ensure that they are stable there at longer mixing times and high screw rotation speeds. Also the mechanical properties of the blends might be weaker because of lack of interfacial adhesion due to short copolymer blocks.

Based on the existence of a shape relaxation at low frequencies for polymer blends, the rheological data of the blends are expected to be sensitive to a change in phase morphology [42,50]. Fig. 13 compares the storage modulus of pure PP and PS homopolymers and PP/PS 50/50 blends with and without compatibilizer at 205 °C. No shear is applied to the blends during measurements. The storage moduli of the blends reveal an excess of elasticity with respect to the neat components. An extra elasticity is clearly visible in the terminal zone, particularly for the compatibilized blends. This excess of elasticity can be explained by the change in the amount of interfacial area during annealing, using the results of Fig. 10.

The elastic moduli of the blends can be modeled in a simple way by decomposing in a bulk and in an interfacial term (Eq. (4)) [48]:

$$G'_{blend} = G'_{components} + G'_{interface} \quad (4)$$

At a certain blend composition, the contribution from the components is constant during the rheological testing while the contribution from the interface changes as the blend morphology changes. Since immiscible polymer blends are not thermodynamically stable, annealing leads to phase coarsening and coalescence. This leads to a decrease in the amount of interface that should be reflected in a decrease in G'.

In uncompatibilized PP/PS 50/50 blends the specific interfacial area, Q is 0.027 μm^{-1}, after 60 min of quiescent annealing at 205 °C (Fig. 10). *In situ* generation of 5 wt% graft copolymer based on PP–MA1 leads to the compatibilization of the blend components with relatively smaller PS phase size (enhancing of the interface, $Q = 0.032\ \mu m^{-1}$), while the contribution from the components at a given composition stays constant. Thus, it is clear that the maximum amount of the interface corresponds to the blend with 5 wt% copolymer based on PP–MA8 with a finer phase morphology

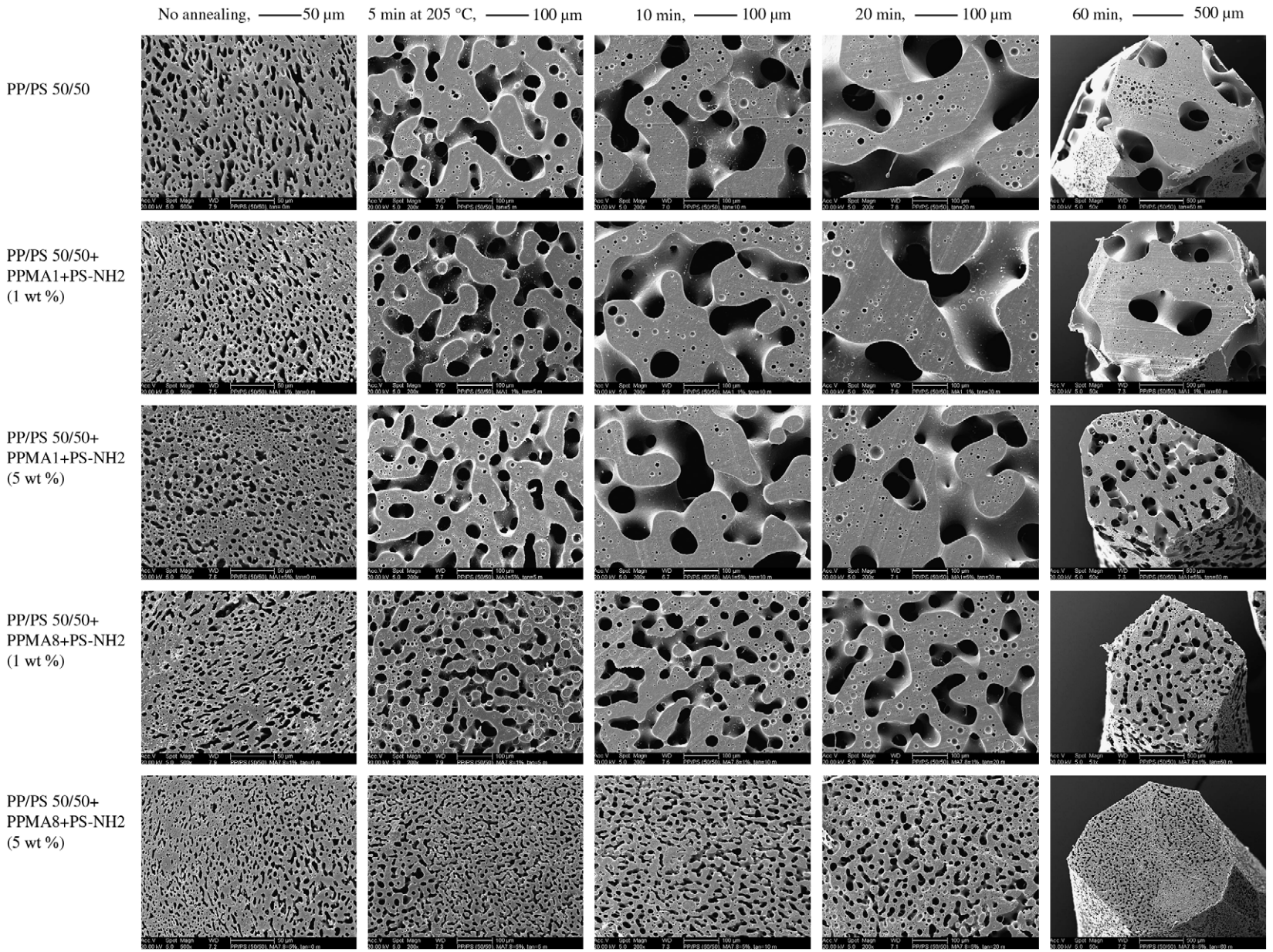

Fig. 9. Phase coarsening during the annealing of uncompatibilized and compatibilized PP12/PS7 50/50 blends at 205 °C.

Table 3
Co-continuity degree, PS phase coarsening rate, and apparent interfacial coverage for uncompatibilized and compatibilized PP/PS 50/50 blends as a function of annealing time

Time of annealing, min (at 205 °C)	(PP/PS)/(PP–MA + PS–NH_2) (wt%)				
	(50/50)/0	(50/50)/1 PP–MA1 based	(50/50)/5 PP–MA1 based	(50/50)/1 PP–MA8 based	(50/50)/5 PP–MA8 based
0	100.0	100.0	99.4	100.0	99.7
5	100.0	100.0	99.6	100.0	98.8
10	100.0	100.0	100.0	100.0	97.8
20	100.0	100.0	97.8	100.0	96.4
90	95.8	95.3	98.6	100.0	98.2
180	95.7	97.9	99.3	99.4	96.5
$c_1\sigma$ [N/m]	1.1×10^{-4}	1.0×10^{-4}	5.7×10^{-5}	4.5×10^{-5}	2.0×10^{-5}
Normalized $c_1\sigma$[a]	1	0.91	0.53	0.41	0.18
Σ, chains/nm^2	–	0.03	0.20	0.13	0.44
(Σ/Σ_{max})[b]	–	0.16	1.01	0.43	1.45

[a] $c_1\sigma$ was normalized with that of the neat blend.
[b] Normalized interfacial coverage.

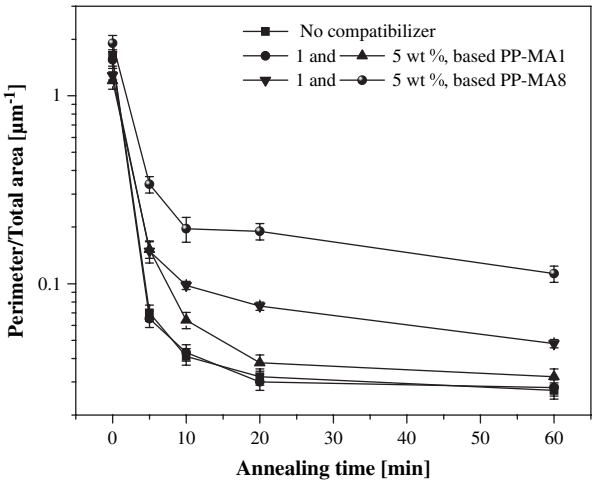

Fig. 10. Specific interfacial area (Q) as a function of annealing time for uncompatibilized and compatibilized PP/PS 50/50 blends at 205 °C.

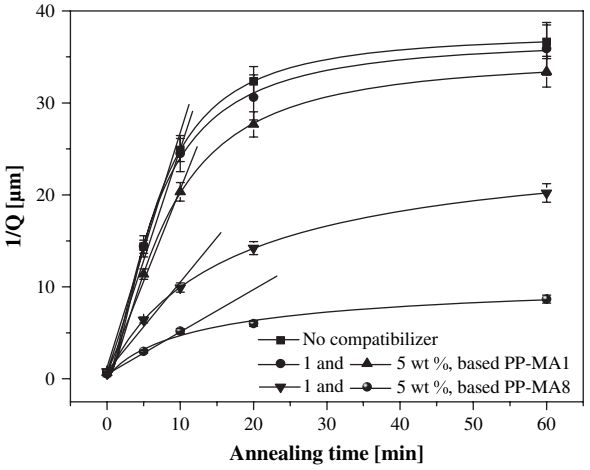

Fig. 11. The reciprocal of the specific interfacial area $1/Q$ as a function of annealing time for uncompatibilized and compatibilized PP/PS 50/50 blends at 205 °C.

and, as a consequence, a higher amount of interface ($Q = 0.113\ \mu m^{-1}$).

4. Conclusions

The phase morphology of PP/PS model blends, uncompatibilized and reactively compatibilized using amino-terminated polystyrene and maleic anhydride grafted polypropylene reactive precursors, is investigated experimentally with particular focus on the behaviour of the co-continuous phase morphology after extrusion.

The onset of PS phase co-continuity depends on the viscosity of both PP and PS phases; increasing the major PP phase viscosity leads to more stable filaments of the minor phase and co-continuity is possible at lower volume fractions. The morphologies within the barrel of the extruder are isotropic, but are subjected to intensive orientation upon passing through the capillary die of the extruder. A co-continuous structure of a 20/80 PP/PS blend with elongated filaments of the PP phase is not stable and can be transformed into a fully dispersed phase morphology after short annealing times.

The structural instability of the phase morphology as a function of the annealing time at a temperature of 205 °C has been studied in uncompatibilized and compatibilized blends with a 50/50 PP/PS composition. The *in situ* generation of 1 and 5 wt% compatibilizer based on PP-*g*-MA1 does not affect the morphology stability significantly. Blends with 5 wt% *in situ* generated compatibilizer based on PP–MA8 precursor cause a reduction of the characteristic phase size of the PS phase suppressing drastically its coarsening.

Acknowledgements

The authors are indebted to the Research Fund of the K.U. Leuven for financial support in the framework of the GOA projects 98/06 and 03/06.

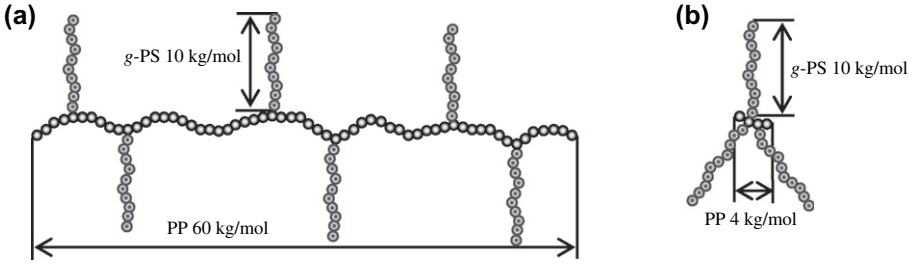

Fig. 12. Architecture and molecular weights of the graft copolymers based on PP–MA1 (a) and PP–MA8 (b) with PS–NH_2.

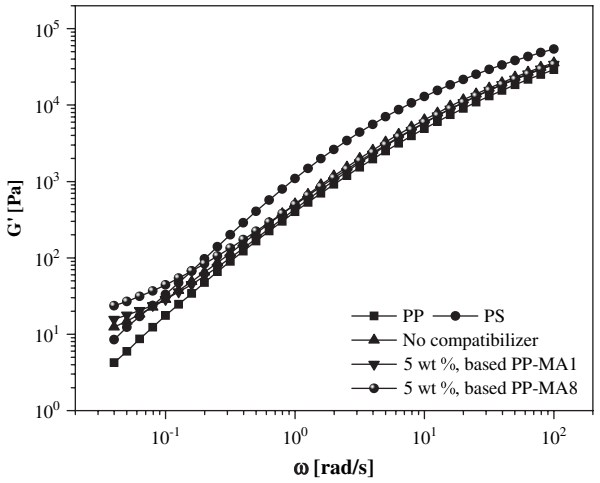

Fig. 13. Storage modulus as a function of frequency for the PP12 and PS7 homopolymers and 50/50 uncompatibilized and compatibilized blends with 5 wt% *in situ* generated compatibilizer based on PP–MA1 and PP–MA8 precursors at 205 °C.

References

[1] Paul DR, Bucknall CB, editors. Polymer blends. New York: Wiley Interscience; 2000 [chapters 15, 22 and 25].
[2] Harrats C, Thomas S, Groeninckx G, editors. Micro- and nanostructured multiphase polymer blend systems: phase morphology and interfaces. USA: CRC Press Taylor & Francis; 2006 [chapters 1–7, 12–13].
[3] Michler GH, Baltá-Calleja FJ, editors. Mechanical properties of polymers based on nanostructure and morphology. Taylor & Francis: CRC Press; 2005.
[4] Avgeropolus GN, Weissert FC, Böhm GGA. Angew Makromol Chem 1977;60/61(4):94.
[5] Paul DR, Barlow JW. J Macromol Sci Rev Macromol Chem 1980;C18:109.
[6] Jordhamo GM, Manson JA, Sperling LH. Polym Eng Sci 1986; 26(8):517–24.
[7] Miles IS, Zurek A. Polym Eng Sci 1988;28(12):796–805.
[8] Ho RM, Wu CH, Su AC. Polym Eng Sci 1990;30(9):511–8.
[9] Kitayama N, Keskkula H, Paul DR. Polymer 2000;41(22):8041–52.
[10] Everaert V, Aerts L, Groeninckx G. Polymer 1999;40(24):6627–44.
[11] Utracki LA. J Rheol 1991;35(8):1615–37.
[12] Utracki LA. Polym Mater Sci Eng 1991;65:50.
[13] Metelkin VI, Blekht VP. Colloid J USSR 1984;46:425.
[14] Harrats C, Omonov TS, Groeninckx G, Moldenaers P. Polymer 2004; 45(24):8115–26.
[15] Harrats C, Fayt R, Jérôme R, Blacher S. J Polym Sci Part B Polym Phys 2003;41(2):202–16.
[16] Quintens D, Groeninckx G, Guest M, Aerts L. Polym Eng Sci 1991; 30(22):1474–83.
[17] Quintens D, Groeninckx G, Guest M, Aerts L. Polym Eng Sci 1991; 30(22):1484–90.
[18] Quintens D, Groeninckx G, Guest M, Aerts L. Polym Eng Sci 1991; 31(16):1207–14.
[19] Quintens D, Groeninckx G, Guest M, Aerts L. Polym Eng Sci 1991; 31(16):1215–21.
[20] Harrats C, Blacher S, Fayt R, Jérôme R, Teyssié Ph. J Polym Sci Polym Phys 1995;33(5):801–11.
[21] Veenstra H, Norder B, van Dam J, Posthuma de Boer A. Polymer 1999;40(18):5223–6.
[22] Willemse RC. Polymer 1999;40(8):2175–8.
[23] Willemse RC, Posthuma de Boer A, van Dam J, Gotsis AD. Polymer 1999;40(4):827–34.
[24] Willemse RC, Posthuma de Boer A, van Dam J, Gotsis AD. Polymer 1998;39(24):5879–87.
[25] Dedecker K, Groeninckx G. Polymer 1998;39(21):4993–5000.
[26] Baker WE, Scott C, Hu GH, editors. Reactive polymer blending. Hanser Gardener Publishers; 2001. p. 48–81 [chapter 3].
[27] Blacher S, Brouers F, Fayt R, Teyssié P. J Polym Sci Part B Polym Phys 1993;B31(6):655–62.
[28] Mekhilef N, Favis BD, Carreau PJJ. J Polym Sci Part B Polym Phys 1997;35(2):293–308.
[29] Verhoogt H, Van Dam J, Posthuma de Boer A. Morphology-processing relationship in interpenetrating polymer blends. In: Klempner D, Sperling LH, Utracki LA, editors. Interpenetrating polymer networks. Washington: Adv Chem Ser 239; 1994. p. 333.
[30] Willemse RC. Formation and stability of co-continuous morphology, PhD Thesis, The Netherlands: TUDelft; 1998.
[31] Veenstra H, Van Dam J, Posthuma de Boer A. Polymer 2000; 41(8):3037–45.
[32] Bourry D, Favis BD. J Polym Sci Part B Polym Phys 1998;36(11): 1889–99.
[33] Li JM, Ma PL, Favis BD. Macromolecules 2002;35(6):2005–16.
[34] Li JM, Ma PL, Favis BD. ANTEC 2001 - proceedings of the 59th annual technical conference & exhibition. Dallas: Society of Plastics Engineers; 2001. p. 1484.
[35] Galloway JA, Jeon HK, Bell JR, Macosko CW. Polymer 2005;46(1): 183–91.
[36] Hietaoja PT, Holsti-Miettinen RM, Seppala JV, Ikkala OT. J Appl Polym Sci 1994;54(11):1613–23.
[37] Willis JM, Caldas V, Favis BD. Mater Sci 1991;26(17):4742–50.
[38] Yuan Z, Favis BD. AIChE J 2005;51(1):271–80.
[39] Lee JK, Han CD. Polymer 1999;40(10):2521–36.
[40] Willemse RC, Ramaker EJJ, Van Dam J, Posthuma De Boer A. Polym Eng Sci 1999;39(9):1717–25.
[41] Doi M, Ohta T. J Chem Phys 1991;95(2):1242–8.
[42] Vinckier I, Laun HM. J Rheol 2001;45(6):1373–85.
[43] Wu S. Polymer interface and adhesion. New York: Marcel Dekker; 1982 [chapter 3].
[44] Omonov TS, Harrats C, Groeninckx G. Polymer 2005;46(26):12322–36.
[45] Berry GC, Fox TG. Adv Polym Sci 1968;5:261–357.
[46] Van Hemelrijck E, Van Puyvelde P, Velankar S, Macosko CW, Moldenaers P. J Rheol 2004;48(1):143–58.
[47] Bates FS, Fredrickson GH. Phys Today 1999;52:32–8.
[48] Galloway JA, Macosko CW. Polym Eng Sci 2004;44(4):714–27.
[49] Braun D, Fisher M, Helmann GP. Polymer 1996;37(17):3871–7.
[50] Vinckier I, Mewis J, Moldenaers P. Rheol Acta 1997;36(5):513–23.